In situ $^{13}CO_2$ labeling reveals that alpine treeline trees allocate less photoassimilates to roots compared to low-elevation trees

Yu Cong[1,2], Matthias Saurer[3], Edith Bai[1], Rolf Siegwolf[3], Arthur Gessler[3,4], Kai Liu[1], Hudong Han[1], Yongcai Dang[1], Wenhua Xu[5,6], Hong S. He[7,1*], Mai-He Li[3,1*]

¹Key Laboratory of Geographical Processes and Ecological Security in Changbai Mountains, *Ministry of Education, School of Geographical Sciences, Northeast Normal University, Changchun 130024, China*

²Northeast Institute of Geography and Agricultural Ecology, Chinese Academy of Sciences, Changchun 130102, China

*³Swiss Federal Institute for Forest, Snow and Landscape Research WSL, Zuercherstrasse*111, *CH-8903 Birmensdorf, Switzerland*

⁴Institute of Terrestrial Ecosystems, ETH Zurich, Universitaetsstrasse 16, 8092 Zurich, Switzerland.

⁵Institute of Agricultural Resource and Environment, Jilin Academy of Agricultural Sciences, Changchun 130033, Jilin, China

⁶CAS Key Laboratory of Forest Ecology and Management, Institute of Applied Ecology, Chinese Academy of Sciences, Shenyang, 110016, China

⁷School of Natural Resources, University of Missouri, Columbia, MO 65211, USA

Correspondence to: Dr. Hong S. He, Dr. Mai-He Li

Tel-Phone: + 573-882-7717; +41447392491

E-mail: heh@missouri.edu; maihe.li@wsl.ch

Abatract

Carbon (C) allocation plays a crucial role for survival and growth of the alpine treeline trees, which, however, is still poorly understood. Using *in situ* $^{13}CO_2$ labeling, we investigated the leaf photosynthesis and the allocation of ^{13}C labeled photoassimilates in various tissues (leaves, twigs and fine roots) in treeline trees and low-elevation trees. Non-structural carbohydrate (NSC) concentrations were also determined. The alpine treeline trees (2000 m. a.s.l.), compared to low-elevation trees (1700 m a.s.l.), did not show any disadvantage in photosynthesis, but the former allocated proportionally less newly assimilated C belowground than the latter. Carbon residence time in leaves was longer in treeline trees (19 d) than that in low-elevation ones (10 d). We found an overall lower density of newly assimilated carbon in treeline trees. The alpine treeline trees may have a photosynthetic compensatory mechanism to counteract the negative effects of the harsh treeline environment (e.g. lower temperature and shorter growing season) on carbon gain. Lower temperature at treeline may limit the sink activity and carbon downward transport via phloem, and shorter treeline growing season may result in early cessation of root growth, decreases sink strength, which all together lead to lower density of new carbon in the sink tissues, and finally limit the growth of the alpine treeline trees.

Introduction

The alpine treeline, the most conspicuous vegetation boundary, is highly sensitive to global and regional environment change (Tranquillini, 1979; Körner, 1999). Trees near the alpine treeline are sensitive to low temperature that limits tree growth (Körner & Paulsen, 2004). Alpine treelines are believed to be associated with a common thermal threshold of $6.7 \pm 0.8°C$ (soil temperature at 10 cm depth) in the growing season (Körner & Paulsen, 2004). The harsh alpine environment characterized by low temperatures, reduced CO_2 pressure, strong winds, and intense UV-radiation (Körner, 1999) may constrain physiological processes that subsequently limit photosynthesis, growth and survival of trees in the alpine treeline ecotone (Tranquillini, 1979). For example, McNown and Sullivan (2013) reported that, compared to low-elevation, white spruce trees at the alpine treeline showed reduced gross and net photosynthesis in northwest Alaska. However, classical gas-exchange studies of the leaves of treeline trees (e.g. *Larix decidua*, *Picea abies*, *Pinus cembra*) have not revealed any particular disadvantages for photosynthesis in these trees compared with those at low altitudes (Tranquillini 1979; Körner 1999).

Photosynthetic carbon gain is only one aspect for the carbon balance of trees; another and probably even more important aspect is how photosynthates are allocated to and invested in various tissues of treeline trees. Tissue levels of non-structural carbohydrates (NSCs) being central for fueling growth, maintenance metabolism and carbon storage capacity, reflect the balance between C assimilation, allocation and consumption within a tree (Körner, 1999; Oleksyn *et al.*, 2000; Hoch *et al.*, 2002; Li *et*

al., 2002; Hoch & Körner, 2003). Two mechanisms might explain increases in tissue NSC concentrations under extreme environmental conditions. On one hand, when growth rather than photosynthesis is constrained by harsh environments, the tissue NSC concentrations often increase passively as carbon supply exceeds demand (Sala *et al.*, 2012; Palacio *et al.*, 2014). On the other hand, to resist environmental stress, e.g. to prevent frost or drought damage, trees growing in severe environmental conditions often actively prioritize C storage and sugar accumulation over growth (Sala *et al.*, 2012; Ouyang *et al.*, 2021), because accumulation of soluble sugars in plant cells is responsible for osmotic adjustment to prevent cell water loss under drought (Woodruff & Meinzer 2011) and/or to prevent intracellular ice formation under sub-zero temperatures (Morin *et al.*, 2007). It is, however, difficult to disentangle whether higher tissue NSC levels are due to lower sink demand than photosynthetic supply or due to an active accumulation for sustaining tree functioning under harsh environmental conditions.

Carbon allocation has been evaluated via biomass partitioning (e.g. Wu *et al.*, 2010) on the long-term and the flux of newly assimilated ^{13}C-labelled carbon to particular plant compartment on the short-term (Epron *et al.*, 2011). Carbon allocation within a whole tree is also affected by environmental conditions (Epron *et al.*, 2012; Joseph *et al.*, 2020), e.g. drought, shading, and nutrient limitation (Giardina *et al.*, 2003; Ruehr *et al.*, 2009; Bahn *et al.*, 2013) as well as species competition (Hommel *et al.*, 2016). Under moderate drought or low nutrient supply conditions, plants increase C allocation to the root system (Poorter *et al.*, 2012), whereas, under low light conditions, they

allocate a relatively higher proportion of assimilated C to shoots, corroborating the 'functional equilibrium hypothesis' (Bloom *et al.*, 1985; Poorter *et al.*, 2012). This hypothesis assumes that growth of those plant organs and tissues is prioritized, which enables the plant to enhance the acquisition of the most limiting resources (Bloom *et al.* 1985; Poorter *et al.* 2012). However, intensive stress conditions damaging a plant can also lead to allocation patterns that oppose the functional equilibrium hypothesis. For example, intensive drought strongly reduces sink activity belowground thus decreasing the carbon demand and consequently leads to reduced belowground allocation of new assimilates (Hagedorn *et al.*, 2016; Joseph *et al.*, 2020).

Thirty years ago, Mordacq *et al.* (1986) already applied $^{13}CO_2$ labelling method to trace and estimate the carbon allocation within young Chestnut trees. However, only few studies found used C-isotope labeling methods to quantitatively analyze carbon allocation and partitioning of newly assimilated C within trees at the alpine treeline. Using $^{13}CO_2$ labeling technique, Kagawa *et al.* (2006) found that a higher proportion of July and August photoassimilate was allocated to belowground parts of *Larix gmelinii* saplings grown in a continuous permafrost zone. In an another treeline labeling experiment with *Pinus mugo*, Ferrari *et al.* (2016) found that trees grown in lower soil temperature allocated less newly assimilated C to roots than those grown in higher soil temperature. Using ^{13}C labelling, Streit *et al.* (2013) found that *Larix decidua* at the treeline showed a limitation of sink activities, reflected by slower C transfer rates belowground relative to lower elevation larch trees. However, recent large-scale NSC-related studies found that both trees (Li *et al.*, 2018) and shrubs (Wang *et al.*, 2021) at

their respective upper limits actively allocate NSC belowground already in summer, in expense of growing season growth, to store NSC for over winter. Therefore, to explain these contrasting results and better understand the mechanisms for treeline formation, it is needed to precisely, quantitatively clarify the carbon production and allocation in treeline trees, using up-to-date methods/techniques.

Hence, in this study, we applied whole tree $^{13}CO_2$ pulse labelling to *Betula ermanii* Cham. trees growing at both the alpine treeline and lower elevation, and tracked the ^{13}C tracer within the plant and transferred to the soil and the atmosphere. We compared $^{13}CO_2$ assimilation and allocation of newly assimilated C between treeline trees (TLTs; 2000 m a.s.l.) and low-elevation trees (LETs; 1700 m a.s.l.) on the Changbai Mountain, northeastern China. Moreover, we determined NSC concentrations in leaves, twigs, and roots. We hypothesize that: (1) treeline trees and low-elevation trees have similar photosynthetic capacity as previously reported (e.g. Tranquillini 1979), but (2) the former allocates proportionally more newly assimilated C to roots than the latter in summer, due to active summer NSC storage in treeline trees recently proposed (Li *et al.*, 2018; Wang *et al.*, 2021), and higher summer root NSC levels found at the treeline trees than the low-elevation ones (Hoch & Körner, 2003).

Materials and methods

Study area

The study was conducted within the Natural Reserve of Changbai Mountain (41°59′N, 127°59′-128°E) in Northeastern China. The area is undisturbed because of its remoteness and high elevation. Vertical spectra of vegetation zones are developed with

7

mixed coniferous broad leaved forests distributed from 740 to 1100 m a.s.l, coniferous forests from 1100 to 1700 m a.s.l, mountain birch forests from 1700 to 1950 m a.s.l, and tundra above 2000 m a.s.l (Yu *et al.*, 2014). The treeline is between 2000 m and 2030 m a.s.l, and was defined as trees with a height of > 3 m and canopy cover of > 20% (Du *et al.*, 2018). The dominant species at the treeline was the deciduous broad-leaved *Betula ermanii*. The climate is temperate continental climate with an annual precipitation ranging from 700 to 1400 mm (Cong *et al.*, 2018), and annual mean growing season (late May – late September) temperature ranging from 3.4 to 8.8°C (mean growing season temperature is 5.9°C) (Cong *et al.*, 2019). Soils were classified as mountain soddy forest soil.

One representative site was selected at 1700 m (low elevation) and 2000 m a.s.l. (treeline elevation) on a west side of Changbai Mountain, respectively. Both sites had the same aspect (west-facing slope) and similar slope angle (~15°). *Betula ermanii* trees in the 1700 m site were naturally generated after a wind disturbance (Jin *et al.*, 2021). Therefore, we could easily find isolated, healthy *B. ermanii* LETs with similar age (approximately 12-yr-old) as target individuals as *B. ermanii* TLTs in the 2000 m site (Fig. 2; Table 1), which provided the opportunity to study differences in partitioning of new assimilates between *B. ermanii* TLTs and LETs without any age effects. The air temperature at the treeline (2000 m a.s.l.) was, on average for the 31 days after pulse labelling (which took place during the growing season at the end of July) 2.5°C lower (Fig. 1a) than at the lower elevation (1700 m a.s.l.). The soil temperature at the treeline was on average by 1.7°C lower than at the lower elevation (Fig. 1b). The mean soil

8

water content at the treeline, probably due to thin soil, stronger wind and solar radiation there, was 33 %, which was clearly lower than that at the lower elevation (mean 42 %) (Fig. 1c).

^{13}C pulse labeling

The ^{13}C pulse labeling was conducted with 4 replicate trees labeled at both elevations on 25 July 2017 (Fig. 2), which was a sunny day. The distance between two neighboring trees was at least 5 m to avoid any potential disturbance on the pulse labeling (An *et al.*, 2015). Two months before isotope labeling, we dug a square trench (hereafter referred to as plot) around each tree with 1.6 m x 1.6 m at 1700 m and 1.4 m x 1.4 m at the treeline elevation, according to crown width and rooting depth. These trenches were packed with polyethylene film and refilled with soil afterwards (Dannoura *et al.*, 2011). The trenches were extended to 30 cm and 20 cm depth at low and treeline elevation, respectively, to cut off roots from plants outside, ensuring all roots and root exudates within the soil originating from the labeled tree, thus avoiding neighboring plants effects on soil respiration.

For the ^{13}C labelling, a chamber was installed around the whole tree crown in each plot on the day before labeling. The chambers made of a steel frame had the following dimensions: 1 m width $\times$ 1 m breadth $\times$ 1.1 m height (Fig. 2). Supported by steel pads, the chamber frames were installed above the forest floor (Fig. 2). Immediately before labelling the top of the chamber was kept open and then sealed with a transparent polyethylene film (more than 90% light transmittance).

We applied antifogging agent on the inside walls of the chamber to reduce water vapor condensation during the ^{13}C pulse labeling, increasing light intensity and reducing $^{13}CO_2$ dissolved in water drops (Fig. 2). The $^{13}CO_2$ was released by injecting 60 ml of 4 mol L^{-1} HCL into 11.94 g solid $Na_2^{13}CO_3$ (99 atom% ^{13}C, Cambridge Isotope Laboratory Inc.). Previous studies suggested that HCL should be added very slowly to avoid or minimize impacts on stomata opening of leaves (An *et al.*, 2015; Keiner *et al.*, 2015; Potthast *et al.*, 2021; Liu *et al.*, 2021). The 60 ml HCL solution was added in 6 times (10 ml each), and each 10 ml was very slowly added with a syringe from outside the chamber into the solid $Na_2^{13}CO_3$ to keep the chamber CO_2 at approximately 600 ppm across the labeling duration of 4 hours. The beaker containing solid $Na_2^{13}CO_3$ was mounted to the steel frame inside the chamber. To guarantee uniform distribution of the $^{13}CO_2$, the air inside the chamber was circulated by four small electric fans (5V, 8 inches in diameter) fixed at the four corners of the chamber (Bahn *et al.*, 2009). During the labeling period, air temperature inside each chamber was stabilized by ice packs mounted in the center of each chamber (Bahn *et al.*, 2013). The temperature inside and outside each chamber was measured during the 4 hour-labelling period, and the air temperature inside chambers at both elevations increased very similarly (Table S1). The CO_2 concentration in the chamber was monitored by an infrared gas analyzer (CIRAS Ⅲ, PP-systems, Amesbury, MA, USA) which detects both $^{12}CO_2$ and $^{13}CO_2$. We took into account that the response of the CIRASⅢ to $^{13}CO_2$ is about 30% lower than to $^{12}CO_2$ (personal information from the manufacturer). Labelling lasted for 4h and the chambers were removed thereafter (Fig. 2).

Sampling and analysis of ^{13}C

Within the 31-day chase period following the ^{13}C pulse labelling, leaves, twigs, roots and soil samples were taken at 4h and 2, 4, 6, 9, 15, 22 and 31 d after the ^{13}C labeling. Additional sampling was performed before labeling (24 July, 2017). At each sampling time, one twig with its attached leaves was taken for leaves and twig samples, and two soil cores with 5 cm in diameter, at a distance of about 20 cm away from the tree stem. These soil samples were collected over the entire depth of the plot (30 cm and 20 cm depth at low and treeline elevation) and pooled thereafter (Ruehr *et al.*, 2009). Roots were separated from the soil with a sieve with a two 2 mm mesh. The sieved soil samples were air-dried and stored at 4 °C, and root samples were washed by wet sieving with a 0.5 mm mesh size to remove attached soil and debris. All leaves, twigs and roots samples were oven-dried at 65 °C for 48 h and ground to fine powder with a ball mill for further analyses (i.e. ^{13}C, NSC). At the end of the experiment, the entire trees were harvested and the biomass of leaves, twigs and roots of each tree was determined. All plant biomass samples were dried for 48 h at 70 °C and weighed for subsequent analyses.

Atmospheric air, foliage- and soil-emitted CO_2 were collected at 4h, and 2, 4, 6, 9, 15, 22 and 31 days after the ^{13}C labeling. Three samples of atmospheric air were gathered with a syringe at about 2 m above the soil surface (Wu *et al.*, 2010). Soil respiration was sampled with opaque PVC chambers (internal diameter 10 cm, height 13 cm). Two opaque PVC collars per plot were permanently installed and pressed into the soil to a depth of 2 cm before the labelling. The collars were closed with chambers

for 30 min to cover the soil surface where living above-ground plants were clipped before (Hafner *et al.*, 2012). Then gas from the chambers was collected after 30 min through rubber pads at the top with a syringe and transferred to gas sampling bags (MBT42-1, Dalian Hede Technology Co., Ltd., Dalian, China). To determine the $\delta^{13}C$ of leaf respired CO_2, air was collected from branch bags. Within each plot, two bags made of opaque polyethylene film were each placed over a branch (Carbone & Trumbore, 2007) and sealed with duct tape for 30 min to let the CO_2 concentration rise. Subsequently, the gas of bags was collected with a syringe and transferred to other gas sampling bags.

The $\delta^{13}C$ values of leaves, twigs, roots and soil samples were measured with an isotope ratio mass spectrometer (Delta V Advantage, Thermo Fisher Scientific Inc., Bremen, Germany) coupled with an elemental analyzer (Flash 2000HT, Thermo Fisher Scientific Inc., Bremen, Germany). Air samples were analyzed for carbon isotope composition and CO_2 concentration with a GC IRMS (Thermo Fisher Precon+GC Box-Delta V Advantage), which was linked to a mass spectrometer (Delta V Advantage, Thermo Fisher Scientific Inc.). The isotope analysis of sample and reference materials was carried out according the recommendations and the identical treatment principle described by Werner and Brand (2001).

Analysis of non-structural carbohydrates

For the extraction, dried and homogenized plant material was mixed with 80 % ethanol, incubated at 80 °C in a water bath shaker for 30 min, and then centrifuged at 4000 rpm

for 10 min. The precipitates were re-extracted twice using 80 % ethanol. The combined supernatants retained to determine soluble sugars by the anthrone method (Dubois *et al.*, 1956). The ethanol-insoluble pellets were used for starch extraction. Starch was extracted from the solid residues after placing in water at 80° C to remove the ethanol. The residues were boiled with 2 ml of distilled water for 15 min. After cooling to room temperature, 2 ml of 9.2 M $HClO_4$ was added for 15 min to hydrolyze the starch. Then 4 ml distilled water was added, and the mixture was centrifuged at 4000 rpm for 10 min. Subsequently, the solid residues were extracted one more time with 2 ml of 4.6 M $HClO_4$ and the hydrolised sugars were determined with the anthrone method. Concentrations were determined at 620 nm using a 721 spectrophotometer (TU-1810, Beijing Purkinje General Instrument Co., Ltd., Beijing, China) (Wang *et al.*, 2017). The concentrations of soluble sugars, starch, and NSC (soluble sugars plus starch) were all expressed on a dry matter basis (% d.m.).

Calculations

^{13}C in samples was expressed as δ^{13}C value (‰), relative to Pee Dee Belemnite (PDB) standard. The isotopic ratio (^{13}C/^{12}C) of each sample R_{sample} was calculated by the following equation (Boutton, 1991; Simard *et al.*, 1997):

$$R_{sample} = \left(\frac{\delta^{13}C}{1000} + 1\right) \times R_{PDB} \qquad (1)$$

$R_{PDB} = 0.011237$ is the isotopic ratio of ^{13}C/^{12}C in PDB.

Atom % (% of ^{13}C in total carbon atoms) of the sample was calculated as follows (Simard *et al.*, 1997):

$$\text{atom\%} = \left(\frac{R_{\text{sample}}}{R_{\text{sample}}+1}\right) \times 100\% \tag{2}$$

The ^{13}C enrichment in different plant organs as a result of the ^{13}C labelling was calculated as ^{13}C atom% excess according to Eqn 3 for total carbon:

$$\text{atom\% excess}^{13}\text{C} = \text{atom\%}_s - \text{atom\%}_b \tag{3}$$

where $\text{atom\%}_s$ and $\text{atom\%}_b$ represent the atom% of the sample at a given time point after labelling and natural abundance sample taken before labelling, respectively.

We applied an indirect method (mass balance method) instead of a direct measurement to obtain $\delta^{13}C_{\text{NSC}}$ (Eqn 4) and estimate the tissue soluble $^{13}C_{\text{excess}}$. We assumed that higher ^{13}C signals (i.e., higher ^{13}C atom %) were due to newly assimilated carbon and thus mainly contributed to NSC. Therefore, the soluble $^{13}C_{\text{excess}}$ of the non-structural carbon was determined with Eqn 5:

$$\delta^{13}C_{\text{NSC}} = \frac{\delta^{13}C_{\text{bulk}} - \delta^{13}C_{\text{unlabeled}} \times (1-[\text{NSC}])}{[\text{NSC}]} \tag{4}$$

$$\text{soluble}^{13}C_{\text{excess}} = \text{atom\%}_{\text{NSC}} - \text{atom\%}_{\text{unlabeled}} \tag{5}$$

where $\delta^{13}C_{\text{bulk}}$ and $\delta^{13}C_{\text{unlabeled}}$ represent the δ^{13}C of bulk labelled sample and unlabeled sample, respectively, and [NSC] is the concentration of non-structural carbohydrates in plant tissues.

The ^{13}C excess pool (mg) in NSC of plant compartments was calculated using Eqn 6, and the area based soluble ^{13}C excess (mg/m^2 projected area) of each compartment (per unit projected area) was calculated according to Eqn 7:

$$\text{soluble}^{13}C_{\text{pool excess}}(\text{mg}) = \frac{\text{soluble}^{13}C_{\text{excess}}}{100} \times \frac{C\ \%}{100} \times \text{DW} \tag{6}$$

$$\text{projected soluble}^{13}C_{\text{excess}}(\text{m g/m}^2) = \frac{\text{soluble}^{13}C_{\text{excess}}}{100} \times \frac{C\ \%}{100} \times B \tag{7}$$

where DW is the dry weight of plant biomass compartments (expressed in mg); B is the dry weight of plant compartments per projected area (expressed in mg m^{-2}); C % is the percentage of C in the sample; the projected area of each plant was determined according to tree crown width.

The δ^{13}C values of foliage and soil respiration were obtained with the following equation (Subke *et al.*, 2004):

$$\delta^{13}C_{respired} = \frac{\delta^{13}C_{chamber} \times [CO_2]_{chamber} - \delta^{13}C_{atmosphere} \times [CO_2]_{atmosphere}}{[CO_2]_{chamber} - [CO_2]_{atmosphere}} \quad (8)$$

where $\delta^{13}C_{chamber}$ and $\delta^{13}C_{atmosphere}$ are the isotopic composition of CO_2 from chamber and ambient atmosphere air, respectively, and $[CO_2]$ is the CO_2 concentration.

To determine mean residence time (MRT) of ^{13}C excess in leaves, the following exponential decay function was fitted (Ruehr *et al.*, 2009):

$$N(t) = N_0 e^{(-\lambda t)} \quad (9)$$

where t is the time in days after the labeling, N_0 is the initial ^{13}C excess at time $t = 0$ directly after labelling (maximum of ^{13}C), λ is the decay constant, and N_t is the amount of ^{13}C after time t. The MRT was then calculated as $1/\lambda$.

Data analysis

Overall differences between TLTs and LETs in size, age and biomass were analyzed using a *t*-test. To test differences in isotopic signature (i.e., ^{13}excess values and soluble ^{13}C excess) between TLTs and LETs, the independent *t*-test was applied at every time-points of ^{13}C dynamics during the 31-day chase period. Mean values and standard errors are given in the tables and figures.

15

Results

Tree size, biomass and photosynthetic capacity

Base diameter, height and the total tree biomass, as well as annual mean tree ring width, were significantly lower in TLTs than in LETs (Table 1; Fig. 3), whereas the maximum photosynthetic rate (A_{max}) and stomatal conductance (gs) were significantly higher in TLTs than in LETs (Table 2). TLTs had significantly higher root-shoot ratio, but similar LMA and total leaf area per tree to LETs (Table 1).

Atom% excess ^{13}C

The ^{13}C atom% excess values in leaves of TLTs were significantly higher than those of LETs ($p < 0.05$) at the majority of the sampling dates (Fig. 4a). At the first sampling date (4 h after the labeling), leaf ^{13}C atom% excess at both elevations reached the highest value and then decreased exponentially over time (Fig. 4a). The decrease rate was slower in TLTs than that in LETs (Fig. 4a), and thus the MRT was higher at the treeline (Table 3). In twigs, ^{13}C atom% excess first increased after labeling and reached its maximum value on the 2nd day (LETs) and 4th day (TLTs) and thereafter it gradually decreased with time (Fig. 4b). It was remarkable that the peak values of twigs in TLTs came later than that in LETs, and then the signal decreased rapidly, but the values of twigs in TLTs and LETs were not different anymore after 22nd day (Fig. 4b). The ^{13}C atom% excess in the fine roots did not differ at any sampling point between TLTs and LETs (Fig. 4c). The maximum ^{13}C atom% excess values in fine roots was

16

found on the 15th day after the labeling in LETs, whereas the peak of the ^{13}C atom% excess in fine roots of TLTs occurred on the 22nd day (7 days later). The ^{13}C excess in soil was generally low and reached its maximum after 4 days at the treeline, but the observed differences between the two elevations in temporal dynamics of ^{13}C excess were not significant (Fig. 4d).

Soluble ^{13}C

Leaf soluble ^{13}C excess (%) calculated according eq. 5 decreased, twig values initially increased and then declined, whereas values in fine roots increased during the sampling period in both TLTs and LETs (Figs. 5a-c). Leaf soluble ^{13}C excess did not differ between TLTs and LETs, except a significantly lower value occurred in TLTs than in LETs on the 31st day after labeling ($p < 0.05$) (Fig. 5a). TLTs tended to have larger soluble ^{13}C excess values in twigs than LETs but a significant difference was found only on the 15th day after pulse labeling ($p < 0.05$) (Fig. 5b). In contrast, the fine root soluble ^{13}C excess seemed to be higher in LETs than in TLTs over the sampling period (Fig. 5c).

The NSC concentrations in leaves and twigs did not vary with the elevation of trees, but TLTs had significantly higher root NSC concentration than LETs (Table 2). An overall trend showed that TLTs had lower levels of the labeled carbon assimilate pool than LETs (Figs. 6a-d). The soluble ^{13}C excess pool in leaves decreased over time (Fig. 6a), whereas values in fine roots tended to increase from the 2nd day to the 31st day after labeling for both LETs and TLTs (Fig. 6c). Twig soluble ^{13}C excess pool in LETs

17

decreased over time, but those of TLTs remained relatively stable after labeling (Fig. 6b). The total soluble ^{13}C excess pool showed comparable steady declining trends in the two elevations (Fig. 6d).

Soluble ^{13}C density per area

Taking into account the differences in tree biomass, we standardized the soluble ^{13}C excess pool values showing in figure 6 based on unit biomass (eq. 6), or unit projected ground surface area (eq. 7). Again, an overall trend was that the soluble ^{13}C density (i.e. per unit projected ground surface area) was lower in TLTs tissues than that in LETs after labeling (Fig. 7a-d). Soluble ^{13}C density showed similar temporal patterns as their soluble ^{13}C excess pool during the sampling period (Fig. 7a-d vs. Fig. 6a-d).

Both leaf respiration and soil respiration of labeled carbon, expressed on the basis of leaf (or plot) area, or of the projected ground surface area, tended to be higher at 1700 m than at the treeline elevation (Fig. 8a-d). There were significantly higher values of leaf respiration ^{13}C excess for LETs on the 2nd day after pulse labeling ($p < 0.05$) (Fig. 8a, c). ^{13}C excess of soil respired CO_2 either per plot (Fig. 8b) or per projected area (Fig. 8d) showed similar temporal patterns for both elevations as their ^{13}C values showed initially a strong increase followed by an asymptotic pattern with time.

Discussion

Temporal patterns showed that ^{13}C from pulse-labelling was immediately incorporated into leaves, and newly formed photosynthates were rapidly transferred

18

from leaves to all tree compartments and to the soil (Figs. 4 and 8). As reported in earlier tree and shrub labelling studies (Ruehr *et al.*, 2009; Anadon-Rosell *et al.*, 2017), we found that the ^{13}C signal in the aboveground components (leaves and twigs) was already present in the first samples collected only few hours after labeling. Moreover, the ^{13}C tracer signal was detected in the fine roots and soil on the 2nd day after labelling (Fig. 4c,d, 8c,d), which demonstrated that new photosynthates were rapidly allocated to the belowground compartment for our sites at 1700 and 2000 m asl (Johnson *et al.*, 2002; Leake *et al.*, 2006). An even faster photosynthetic ^{13}C translocation to roots within 1 day after labeling was found in saplings (Blessing *et al.*, 2015). Ruehr *et al* (2009) found that recently assimilated C allocated to roots and soil within 1 day after labeling, whereas it took 6 days until the label arrived in the aboveground compartment in 10- to 15-m-tall Scots pine in a dry area (Jospeh *et al.*, 2020).

TLTs sustained a relatively high level of maximum photosynthetic rate ($A_{\max}$) (Table 2), and consequently ^{13}C maximum peak in leaves of the two elevations were comparable, even with a trend to higher soluble ^{13}C excess values in leaves and twigs of TLTs ($p < 0.05$) (Figs. 5a, b), indicating that the lower temperatures at the treeline (Fig. 1a) did not negatively affect photosynthesis. Our findings differ from those of McNown and Sullivan (2013), who found that white spruce trees at the treeline showed reduced gross and net photosynthesis in northwest Alaska. In contrast, and in line with our findings, Körner and Diemer (1987) observed that in plants from high altitude exposed to low-temperature, net photosynthetic rates were not significantly reduced compared to those from lower altitude during the growing season. Lower growth often

observed at tree-line trees, as also observed in our study, may be rather due to a shorter

growing season and reduced sink activity, and not due to reduced photosynthesis. It

was, thus, observed that cessation of structural growth was correlated with phenology

(season length) (Körner, 2015), which inevitably led to treeline plants growing slower

than lowland plants. Furthermore, sink activity may be more constrained than

photosynthesis by low temperature (Körner, 1999), as plant metabolism and microbial

activity were tightly related to temperature (Zhu *et al.*, 2012a, b).

TLTs showed a slower decrease of ^{13}C excess in leaves compared to LETs (Fig. 4a),

reflected by longer MRT of labelled carbon in leaves (Table 3), and thus the peak of

^{13}C excess in twigs and fine roots of TLTs occurred later than that of LETs (Fig. 4b-c).

These patterns might indicate a reduced sink activity and thus lower growth in TLTs

under lower temperature (Table 1). However, it is difficult to disentangle whether the

carbon accumulation in leaves is caused by lower sink activity or lower phloem

transport or a combination of both. Similar result had been found in an earlier study, in

which lower temperature decreased root turnover (Pregitzer *et al.*, 2000). In addition,

we found that TLTs had a narrower tree ring width (Fig. 3), representing a lower growth

rate, which further corroborated our assumption of sink limitation. We, however,

acknowledge that narrower tree rings could be also a result of a shorter growing season

rather than reduced growth at a given time point during the season. However, it has

been shown that growth rate is low under low temperature despite a relative high

availability of photoassimilates (Körner, 2015). When growth is slow or cessative,

plants commonly reveal a carbon overflow (photosynthesis exceeding growth) (Körner,

2003), leading to an accumulation of non-used assimilates in sink tissues and reduced export from photosynthetically active source tissues (Hagedorn *et al.*, 2016). Thus, the slower transfer of carbon observed in the TLTs might reflect such an oversupply of photosynthates at the treeline. This interpretation is supported by results of a study, in which *Larix decidua* at the treeline revealed slower C transfer rates relative to lowland larch (Streit *et al.*, 2013).

We acknowledge that phloem transport rate might also be directly reduced by low temperature (Wardlaw & Bagnall, 1981; Lemoine *et al.*, 2013), which, however, may not be the case in the present study, because the air temperature did not differ between TLTs and LETs (Fig. 1a), and the lower soil temperature for TLTs were still relatively high (>14°C; Fig. 1b). On the other hand, we speculate that the lower soil moisture at the treeline (Fig. 1c) might increase the fluid viscosity and thus decrease the phloem transport velocity in TLTs. Moreover, an alternative explanation may be the difference in root phenology between TLTs and LETs, as roots of LETs were still in the active growth stage and LETs were still in the phase of active basipetal phloem translocation, while TLTs were closer to the end of the growing season with slow fine root growth rate and their roots were already filled with stored carbohydrates (Table 2), due to active summer carbon storage (Li *et al.*, 2018; Wang *et al.*, 2021).

However, there is increasing indication in recent literature that carbon allocation in plants is strongly sink driven and directly controlled by environmental factors (Bahn *et al.*, 2013; Epron *et al.*, 2012; Joseph *et al.*, 2020). The treeline trees had higher soluble ^{13}C excess in leaves and twigs (Fig. 5a,b) but lower soluble ^{13}C excess in roots (Fig. 5c)

than the low-elevation trees, indicating that the treeline trees have less efficiency to allocate new assimilates belowground. These results are consistent with previous studies that demonstrated lower NSC concentrations in roots of trees and shrubs at their upper limits compared to lower elevations (e.g. Li *et al.*, 2008a, b; Zhu *et al.*, 2012b; Li *et al.*, 2018; Wang *et al.*, 2021). The low soluble ^{13}C incorporation by treeline roots might be attributed to a lower demand for root growth (i.e. sink activity) or a limited downward phloem carbon transport or both. Furthermore, low soluble ^{13}C in roots might also be a result of direct utilization of NSC for rhizodeposition (Hafner *et al.*, 2012), which is illustrated by the large ^{13}C excess amounts in the soil (Fig. 4d). Moreover, although the treeline trees had smaller size (biomass, leaf area, crown-projected area) (Table 1, Fig. 2) but higher photosynthetic capacity (Table 2) than the low-elevation ones, the standardized (i.e. area-based) soluble ^{13}C excess in tissues was lower in trees at the treeline than at the low-elevation (Fig 7). These results suggest that the treeline trees, compared to the low-elevation trees, have less carbon available for growth.

In contrast with the reduced belowground transport in TLTs than LETs, the root NSC concentration was measured to be significantly higher in the former than the latter during the study period from end-July to end-August (Table 2). In this time period, roots of trees at the upper limit (i.e. TLTs) and at lower elevations (e.g. LETs) within the treeline ecotone may face different phenological stages, as LETs were still in the phase of active basipetal phloem translocation, while roots of TLTs were already filled with stored carbohydrates, leading to higher root NSC concentrations in TLTs than LETs

(Table 2). Moreover, the root NSC measured (Table 2) may also include both "old" and "new" NSC. Previous studies indicated that root NSC showed a carbon age of > 10 years (Carbone *et al.*, 2013; Richardson *et al.*, 2015), while soluble ^{13}C measured (Figs. 4 - 8) was the "new" NSC only. Therefore, we believe that this high root NSC concentration in TLTs may be the results of long-term accumulation (i.e., old NSC) and further also due to active carbon storage (i.e., new NSC) (Li *et al.* 2018; Wang *et al.*, 2021) at the expense of growth during the growing season (Li & Yang, 2004; Li *et al.*, 2003), ensuring the trees' survival in the harsh treeline environment. This carbohydrate storage is crucial for regrowth of new leaves in a leafless state of deciduous trees in early spring (Marchi *et al.*, 2005a, b; Zhu *et al.*, 2012a). As a result of seasonal asynchronicity between C supply and demand, C storage serves as a buffer pool to cope with the imbalance of supply and demand (Fischer & Höll, 1991; Newell *et al.*, 2002). As previously reported for deciduous species (Chapin *et al.*, 1990), carbon compounds are stored in ligneous tissues, particularly in stems and roots (Chapin 1980). Moreover, a recent study corroborated this hypothesis by the finding that woody roots and stems of *B. ermanii* trees at high elevation are the most important storage tissues for carbohydrates over winter (Cong *et al.*, 2019).

Conclusions

In line with our 1st hypothesis, we found that the treeline trees did not show any disadvantage in assimilation compared to low-elevation trees, indicating a photosynthetic compensatory mechanism of trees growing in harsh environment with

23

lower temperature. Although the elevational difference was 300 m only (1700 m vs. 2000 m a.s.l.), we did find, contrary to our 2nd hypothesis, that treeline trees proportionally allocate less newly assimilated C belowground than low-elevation trees, which may be a combined result of the differences in sink activity, phloem carbon transport velocity, and root phenological stages caused by different growth conditions (mainly temperature and soil water conditions) between the treeline trees and low-elevation trees. The present study indicated an overall trend that the treeline tree tissues had a lower soluble ^{13}C density (i.e., per unit projected ground surface area) of newly assimilated carbon than the low-elevation tree tissues. This provides new insights into the carbon-physiological mechanisms for the alpine treeline formation, and provide carbon-physiological evidence for recent findings that lower growth rate (Ren *et al.*, 2019) caused by low carbon density in combination with shorter growing season length associated with temperature (Gao *et al.*, 2022) co-determine the high-elevation tree growth. We, therefore, conclude that a low soluble carbon density during the shorter growing season is a primary control of the alpine treeline formation. Moreover, the present study will also contribute to precisely predict the alpine treeline dynamics in response to longer growing season associated with currently rapid climate warming.

Data and Materials Availability

For manuscripts that are accepted, all authors agree to make experimental data and materials available to third party academic researchers upon reasonable request.

Conflict of Interest

The authors declared that they have no conflicts of interest to this work. We declare that we do not have any commercial or associative interest that represents a conflict of interest in connection with the work submitted.

Funding

Acknowledgements

Authors' contributions

H. He, E. Bai, MH Li and Y. Cong conceived the ideas; MH Li, H. He, Y. Cong and W. Xu designed the experiment; K. Liu, H. Han, Y. Dang and Y. Cong performed the research; Y. Cong analyzed the data and wrote the manuscript; M. Saurer, MH Li, E. Bai, R. Siegwolf and A. Gessler commented and revised the manuscript.

References

An T, Schaeffer S, Li S, Fu S, Pei J, Li H, Zhuang J, Radosevich M, Wang J. 2015. Carbon fluxes from plants to soil and dynamics of microbial immobilization under plastic film mulching and fertilizer application using ^{13}C pulse-labeling. *Soil Biology & Biochemistry* **80**: 53-61.

Anadon-Rosell A, Hasibeder R, Palacio S, Mayr S, Ingrisch J, Ninot JM, Nogués S, Bahn M. 2017. Short-term carbon allocation dynamics in subalpine dwarf shrubs and their responses to experimental summer drought. *Environmental and experimental botany* **141**: 92-102.

Bahn M, Schmitt M, Siegwolf R, Richter A, Brüggemann N. 2009. Does photosynthesis affect grassland soil-respired CO_2 and its carbon isotope composition on a diurnal timescale? *New Phytologist* **182**: 451–460.

Bahn M, Lattanzi FA, Hasibeder R, Wild B, Koranda M, Danese V, Brüggemann N, Schmitt M, Siegwolf R, Richter A. 2013. Responses of belowground carbon allocation dynamics to extended shading in mountain grassland. *New Phytologist* **198**: 116-126.

Blessing CH, Werner RA, Siegwolf R, Buchmann N. 2015. Allocation dynamics of recently fixed carbon in beech saplings in response to increased temperatures and drought. *Tree Physiology* **35**: 585-598.

Bloom AJ, Chapin III FS, Mooney HA. 1985. Resource limitation in plants-an economic analogy. *Annual review of Ecology and Systematics* **16**: 363-392.

Boutton TW, 1991. Stable carbon isotope ratios of natural materials: I. Sample preparation and mass spectrometric analysis. In: DC Coleman and B. Fry (Editors), Carbon Isotope Techniques. Academic Press, San Diego, CA, pp. 155-171.

Carbone MS, Trumbore SE. 2007. Contribution of new photosynthetic assimilates to respiration by perennial grasses and shrubs: residence times and allocation patterns. *New Phytologist* **176**, 124-135.

Carbone MS, Czimczik CI, Keenan TF, Murakami PF, Pederson N, Schaberg PG, Xu X, Richardson AD. 2013. Age, allocation and availability of nonstructural carbon in mature red maple trees. *New Phytologist* **200**, 1145-1155.

Chapin F. 1980. The mineral nutrition of wild plants. *Annual review of ecology and systematics* **11**: 233-260.

Chapin F, Schulze E-D, Mooney HA. 1990. The Ecology and Economics of Storage in Plants. *Annual Review of Ecology and Systematics* **21**: 423-447.

Cong Y, Wang A, He H, Yu F, Tognetti R, Cherubini P, Wang X, Li MH. 2018. Evergreen *Quercus aquifolioides* remobilizes more soluble carbon components but less N and P from leaves to shoots than deciduous *Betula ermanii* at the end-season. *iForest-Biogeosciences and Forestry* **11**: 517–525.

Cong Y, Li M-H, Liu K, Dang Y-C, Han H-D, He HS. 2019. Decreased Temperature with Increasing Elevation Decreases the End-Season Leaf-to-Wood Reallocation of Resources in Deciduous *Betula ermanii* Cham. Trees. *Forests* **10**: 166.

Dannoura M, Maillard P, Fresneau C, Plain C, Berveiller D, Gerant D, Chipeaux C, Bosc A, Ngao J, Damesin C. 2011. *In situ* assessment of the velocity of carbon

transfer by tracing ^{13}C in trunk CO_2 efflux after pulse labelling: variations among tree species and seasons. *New Phytologist* **190**: 181-192.

Du H, Liu J, Li MH, Büntgen U, Yang Y, Wang L, Wu Z, He HS. 2018. Warming-induced upward migration of the alpine treeline in the Changbai Mountains, northeast China. *Global Change Biology* **24**: 1256-1266.

Dubois M, Gilles KA, Hamilton JK, Rebers P, Smith F. 1956. Colorimetric method for determination of sugars and related substances. Analytical Chemistry, **28**: 350-356.

Epron D, Ngao J, Dannoura M, Bakker MR, Zeller B, Bazot S, Bosc A, Plain C, Lata JC, Priault P. 2011. Seasonal variations of belowground carbon transfer assessed by in situ $^{13}CO_2$ pulse labelling of trees. *Biogeosciences* **8**: 1153-1168.

Epron D, Bahn M, Derrien D, Lattanzi FA, Pumpanen J, Gessler A, Högberg P, Maillard P, Dannoura M, Gérant D. 2012. Pulse-labelling trees to study carbon allocation dynamics: a review of methods, current knowledge and future prospects. *Tree Physiology*, **32**, 776-798.

Ferrari A, Hagedorn F, Niklaus P. 2016. Experimental soil warming and cooling alters the partitioning of recent assimilates: evidence from a ^{14}C-labelling study at the alpine treeline. *Oecologia* **181**: 25-37.

Fischer C, Höll W. 1991. Food reserves of Scots pine (*Pinus sylvestris* L.). *Trees* **5**: 187-195.

Gao S, Liang EY, Liu RS, Babst F, Camarero J, Fu YS, Piao SL, Rossi S, Shen MG, Wang T, Peñuelas J. 2022. An earlier start of the thermal growing season enhances

tree growth in cold humid areas but not in dry areas. *Nature Ecology and Evolution.* DOI: 10.1038/s41559-022-01668-4

Giardina CP, Ryan MG, Binkley D, Fownes JH. 2003. Primary production and carbon allocation in relation to nutrient supply in a tropical experimental forest. *Global Change Biology* **9**: 1438-1450.

Hafner S, Unteregelsbacher S, Seeber E, Lena B, Xu X, Li X, Guggenberger G, Miehe G, Kuzyakov Y. 2012. Effect of grazing on carbon stocks and assimilate partitioning in a Tibetan montane pasture revealed by $^{13}CO_2$ pulse labeling. *Global Change Biology* **18**: 528-538.

Hagedorn F, Joseph J, Peter M, Luster J, Pritsch K, Geppert U, Kerner R, Molinier V, Egli S, Schaub M, Liu JF, Li MH, Sever K, Weiler M, Siegwolf RTW, Gessler A, Arend M. 2016. Recovery of trees from drought depends on belowground sink control. *Nature Plants* **2**: 16111.

Hoch G, Körner C. 2003. The carbon charging of pines at the climatic treeline: a global comparison. *Oecologia* **135**: 10-21.

Hoch G, Popp M, Körner C. 2002. Altitudinal increase of mobile carbon pools in *Pinus cembra* suggests sink limitation of growth at the Swiss treeline. *Oikos* **98**: 361-374.

Jin Y, Xu J, He H, Tao Y, Wang H, Zhang Y, Hu R, Gao X, Bai Y, Zhao C, Shui X, Li MH. 2021. Effects of catastrophic wind disturbance on formation of forest patch mosaic structure on the western and southern slopes of Changbai Mountain. *Forest Ecology and Management **481***: 118746.

Johnson D, Leake J, Ostle N, Ineson P, Read D. 2002. *In situ* $^{13}CO_2$ pulse‑labelling of upland grassland demonstrates a rapid pathway of carbon flux from arbuscular mycorrhizal mycelia to the soil. *New Phytologist* **153**: 327-334.

Joseph J, Gao D, Backes B, Bloch C, Brunner I, Gleixner G, Haeni M, Hartmann H, Hoch G, Hug C et al. 2020. Rhizosphere activity in an old-growth forest reacts rapidly to changes in soil moisture and shapes whole-tree carbon allocation. *Proceedings of the National Academy of Sciences*, **117**: 24885-24892.

Kagawa A, Sugimoto A, Maximov TC. 2006. Seasonal course of translocation, storage and remobilization of ^{13}C pulse-labeled photoassimilate in naturally growing *Larix gmelinii* saplings. *New Phytologist*, **171**: 793-804.

Keiner R, Gruselle MC, Michalzik B, Popp J, Frosch T. 2015. Raman spectroscopic investigation of $^{13}CO_2$ labeling and leaf dark respiration of *Fagus sylvatica* L. (European beech). *Analytical and Bioanalytical Chemistry* **407**: 1813–1817.

Körner C. 1998. A re-assessment of high elevation treeline positions and their explanation. *Oecologia* **115**: 445-459.

Körner C. 1999. *Alpine Plant Life: Functional Plant Ecology of High Mountain Ecosystems*. Berlin, Gemany: Spinger.

Körner C. 2003. Carbon limitation in trees. *Journal of ecology* **91**: 4-17.

Körner C. 2015. Paradigm shift in plant growth control. *Current opinion in plant biology* **25**: 107-114.

Körner C, Diemer M. 1987. *In situ* photosynthetic responses to light, temperature and carbon dioxide in herbaceous plants from low and high altitude. *Functional Ecology* **1**: 179-194.

Körner C, Paulsen J. 2004. A world‐wide study of high altitude treeline temperatures. *Journal of Biogeography* **31**: 713-732.

Leake JR, Ostle NJ, Rangel-Castro JI, Johnson D. 2006. Carbon fluxes from plants through soil organisms determined by field $^{13}CO_2$ pulse-labelling in an upland grassland. *Applied Soil Ecology* **33**: 152-175.

Lemoine R, La Camera S, Atanassova R, Dedaldechamp F, Allario T, Pourtau N, Bonnemain J-L, Laloi M, Coutos- Thévenot P, Maurousset L, Faucher M, Girousse C, Lemonnier P, Parrilla J, Durand M. 2013. Source-to-sink transport of sugar and regulation by environmental factors. *Frontiers in Plant Science* **4**: 272.

Li MH, Yang J. 2004. Effects of microsite on growth of Pinus cembra in the subalpine zone of the Austrian Alps. *Annals of Forest Science* **61**: 319-325.

Li MH, Hoch G, Körner C. 2002. Source/sink removal affects mobile carbohydrates in *Pinus cembra* at the Swiss treeline. *Trees* **16**: 331-337.

Li MH, Yang J, Kräuchi N. 2003. Growth responses of *Picea abies* and *Larix decidua* to elevation in subalpine areas of Tyrol, Austria. *Canadian Journal of Forest Research* **33**: 653-662.

Li MH, Xiao WF, Shi PL, Wang SG, Zhong YD, Liu XL, Wang XD, Cai XH, Shi ZM. 2008a. Nitrogen and carbon source–sink relationships in trees at the Himalayan treelines compared with lower elevations. *Plant, Cell & Environment* **31**: 1377-1387.

Li MH, Xiao W, Wang S, Cheng G, Cherubini P, Cai X, Liu X, Wang X, Zhu W. 2008b. Mobile carbohydrates in Himalayan treeline trees I. Evidence for carbon gain limitation but not for growth limitation. Tree Physiology **28**: 1287-1296.

Li MH, Jiang Y, Wang A, Li X, Zhu W, Yan C-F, Du Z, Shi Z, Lei J, Schönbeck L. 2018. Active summer carbon storage for winter persistence in trees at the cold alpine treeline. *Tree physiology* **38**: 1345-1355.

Liu ZW, Wu XL, Li SX, Liu W, Bian RJ, Zhang XH, Zheng JF, Drosos M, Li LQ, Pan GX, 2021. Quantitative assessment of the effects of biochar amendment on photosynthetic carbon assimilation and dynamics in a rice–soil system. *New Phytologist* **232**: 1250-1258.

Marchi S, Sebastiani L, Gucci R, Tognetti R. 2005a. Changes in sink-source relationships during shoot development in olive. *Journal of the American Society for Horticultural Science* **130**: 631-637.

Marchi S, Sebastiani L, Gucci R, Tognetti R. 2005b. Sink-source transition in peach leaves during shoot development. *Journal of the American Society for Horticultural Science* **130**: 928-935.

McNown RW, Sullivan PF. 2013. Low photosynthesis of treeline white spruce is associated with limited soil nitrogen availability in the Western Brooks Range, Alaska. *Functional Ecology* **27**: 672-683.

Mordacq L, Mousseau M, Deleens E. 1986. A ^{13}C method of estimation of carbon allocation to roots in a young chestnut coppice. *Plant Cell & Environment* **9**:735–739.

Morin X, Améglio T, Ahas R, Kurz-Besson C, Lanta V, Lebourgeois F, Miglietta F, Chuine I. 2007. Variation in cold hardiness and carbohydrate concentration from dormancy induction to bud burst among provenances of three European oak species. *Tree Physiology* **27**: 817-825.

Newell EA, Mulkey SS, Wright JS. 2002. Seasonal patterns of carbohydrate storage in four tropical tree species. *Oecologia* **131**: 333-342.

Oleksyn J, Zytkowiak R, Karolewski P, Reich P, Tjoelker M. 2000. Genetic and environmental control of seasonal carbohydrate dynamics in trees of diverse *Pinus sylvestris* populations. *Tree Physiology* **20**: 837-847.

Ouyang S, Gessler A, Saurer M, Hagedorn F, Gao DC, Wang XY, Schaub M, Li MH, Shen WJ, Schonbeck L. 2021. Root carbon and nutrient homeostasis determines downy oak sapling survival and recovery from drought. *Tree physiology*. doi:10.1093/treephys/tpab019.

Palacio S, Hoch G, Sala A, Körner C, Millard P. 2014. Does carbon storage limit tree growth? *New Phytologist* **201**: 1096-1100.

Poorter H, Niklas KJ, Reich PB, Oleksyn J, Poot P, Mommer L. 2012. Biomass allocation to leaves, stems and roots: meta‐analyses of interspecific variation and environmental control. *New Phytologist* **193**: 30-50.

Potthast K, Meyer S, Tischer A, Gleixner G, Sieburg A, Frosch T, Michalzik B. 2021. Grasshopper herbivory immediately affects element cycling but not export rates in an N-limited grassland system. *Ecosphere* **12**: e03449.

Pregitzer KS, King JS, Burton AJ, Brown SE. 2000. Responses of tree fine roots to temperature. *The New Phytologist* **147**: 105-115.

Ren P, Ziaco E, Rossi S, Biondi F, Prislan Peter, Liang EY. 2019. Growth rate rather than growing season length determines wood biomass in dry environments. *Agricultural and forest meteorology* **271**: 46-53.

Richardson AD, Carbone MS, Huggett BA, Furze ME, Czimczik CI, Walker JC, Xu X, Schaberg PG, Murakami P. 2015. Distribution and mixing of old and new nonstructural carbon in two temperate trees. *New Phytologist* **206**: 590-597.

Ruehr NK, Offermann CA, Gessler A, Winkler JB, Ferrio JP, Buchmann N, Barnard RL. 2009. Drought effects on allocation of recent carbon: from beech leaves to soil CO2 efflux. *New Phytologist* **184**: 950-961.

Sala A, Woodruff DR, Meinzer FC. 2012. Carbon dynamics in trees: feast or famine? *Tree Physiology* **32**: 764-775.

Simard SW, Durall DM, Jones MD. 1997. Carbon allocation and carbon transfer between *Betula papyrifera* and *Pseudotsuga menziesii* seedlings using a ^{13}C pulse-labeling method. *Plant and Soil* **191**: 41-55.

Streit K, Rinne KT, Hagedorn F, Dawes MA, Saurer M, Hoch G, Werner RA, Buchmann N, Siegwolf RT. 2013. Tracing fresh assimilates through *Larix decidua* exposed to elevated CO_2 and soil warming at the alpine treeline using compound‑specific stable isotope analysis. *New Phytologist* **197**: 838-849.

Subke JA, Hahn V, Battipaglia G, Linder S, Buchmann N, Cotrufo MF. 2004. Feedback interactions between needle litter decomposition and rhizosphere activity. *Oecologia* **139**: 551-559.

Tranquillini W. 1979. *Physiological ecology of the alpine timberline. Tree existence at high altitudes with special references to the European Alps*. New York , UK: Springer-Verlag.

Wang X, Yu FH, Jiang Y, Li MH. 2021. Carbon and nutrient physiology in shrubs at the upper limits: a multi-species study. *Journal of Plant Ecology* **14**: 301-309.

Wardlaw, I. F., Bagnall, D. 1981. Phloem transport and the regulation of growth of *Sorghum bicolor* (Moench) at low temperature. *Plant Physiology* **68**: 411-414.

Werner RA, Brand WA. 2001. Referencing strategies and techniques in stable isotope ratio analysis. *Rapid Communications in Mass Spectrometry* **15**: 501-519.

Wu Y, Tan H, Deng Y, Wu J, Xu X, Wang Y, Tang Y, Higashi T, Cui X. 2010. Partitioning pattern of carbon flux in a Kobresia grassland on the Qinghai-Tibetan Plateau revealed by field ^{13}C pulse-labeling. *Global Change Biology* **16**: 2322–2333.

Woodruff DR, Meinzer FC. 2011. Water stress, shoot growth and storage of non-structural carbohydrates along a tree height gradient in a tall conifer. *Plant, Cell & Environment* **34**: 1920-1930.

Yu D, Wang Q, Liu J, Zhou W, Qi L, Wang X, Zhou L, Dai L. 2014. Formation mechanisms of the alpine Erman's birch (*Betula ermanii*) treeline on Changbai Mountain in Northeast China. *Trees* **28**: 935-947.

Zhu W, Xiang J, Wang S, Li M. 2012a. Resprouting ability and mobile carbohydrate reserves in an oak shrubland decline with increasing elevation on the eastern edge of the Qinghai–Tibet Plateau. *Forest Ecology and Management* **278**: 118-126.

Zhu WZ, Cao M, Wang SG, Xiao WF, Li MH. 2012b. Seasonal dynamics of mobile carbon supply in *Quercus aquifolioides* at the upper elevational limit. PLoS ONE **7**: e34213.
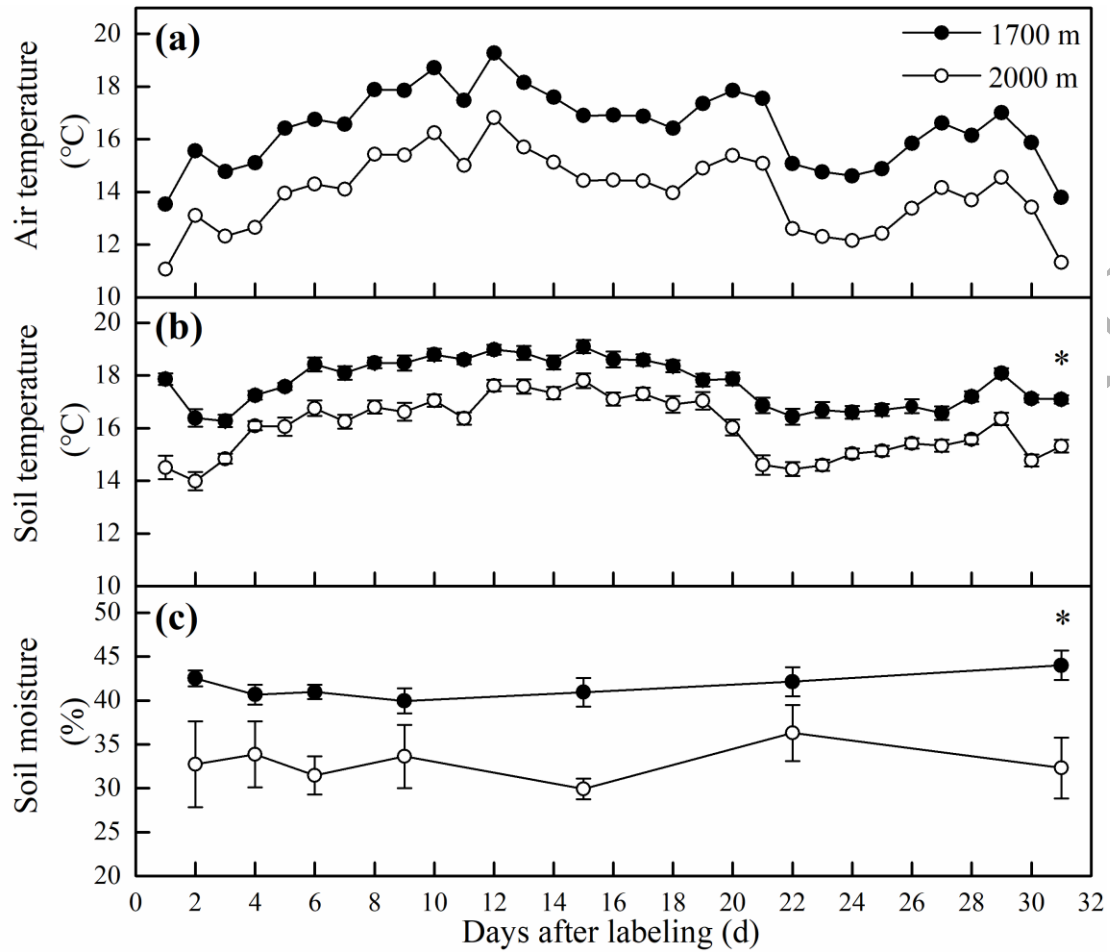
Figure legends

Fig. 1. Dynamics of mean daily air temperature (a), mean daily soil temperature (b) and

average soil moisture (c) (Mean ± SE) during the ^{13}C pulse labeling (n=4 per elevation).

* denotes overall significant differences at $p < 0.05$ between the 1700 m and 2000 m
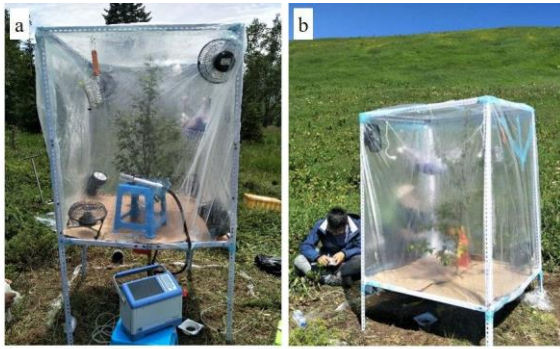
plots.

Fig. 2. Pictures of the labeling experimental set-up at the low-elevation (a, 1700 m) and treeline (b, 2000 m a.s.l.) plots on Changbai Mountain.
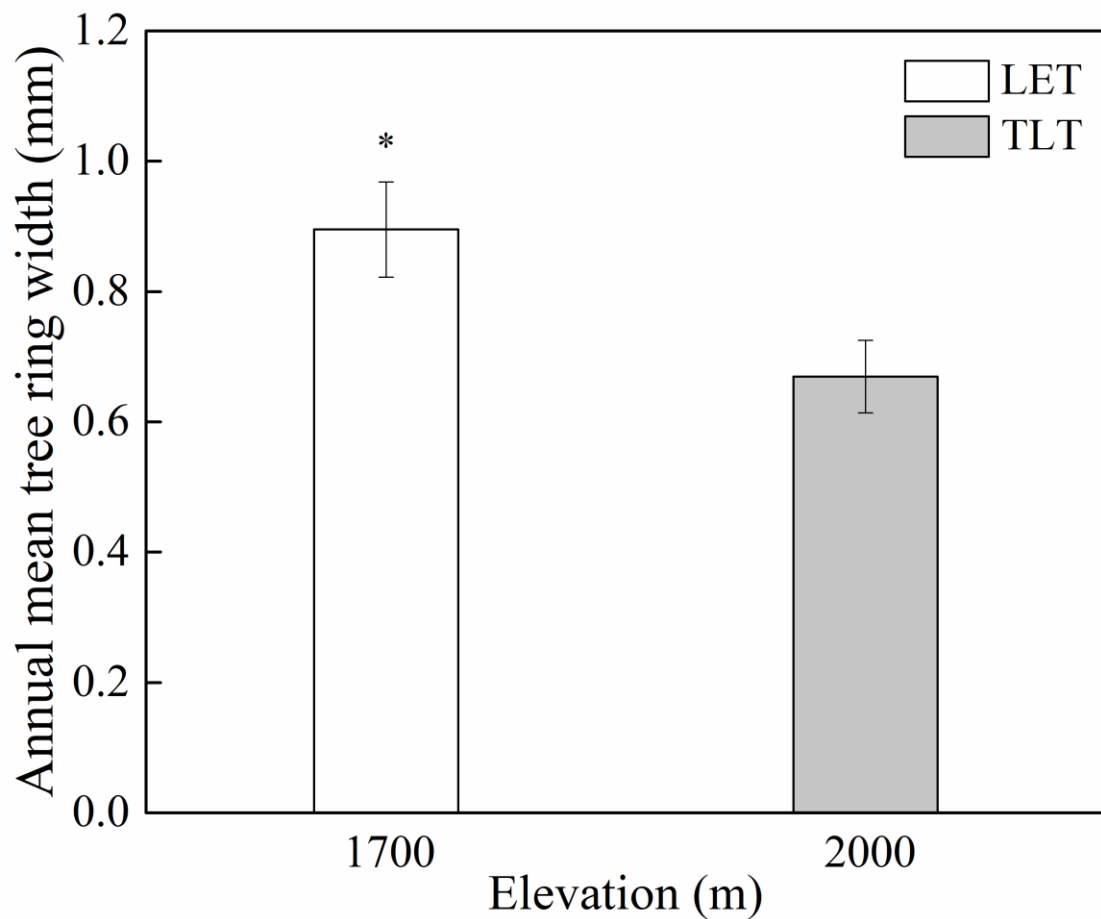

Fig. 3. Annual mean tree ring width of *Betula ermanii* trees (mean ± SE, n=4 trees for each elevation plot) at 1700 m and 2000 m a.s.l. (treeline). * denotes significant differences (*T*-test, $p < 0.05$) between the 1700 m and 2000 m plots.
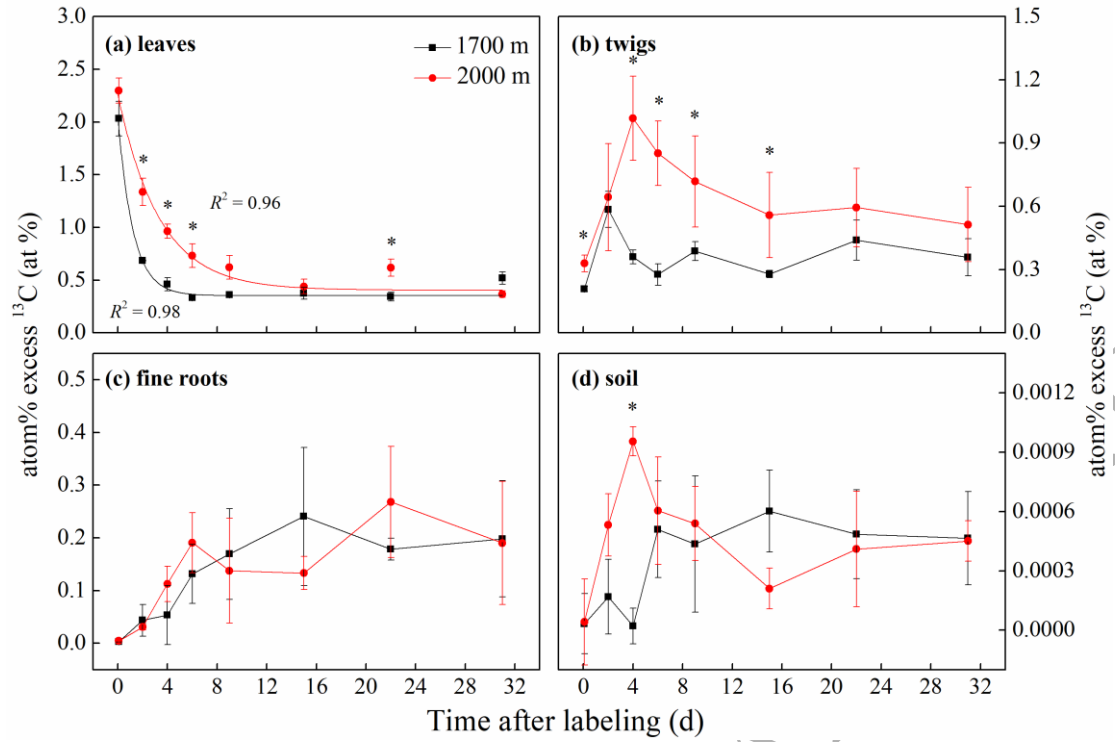
Fig. 4. Temporal variation of ^{13}C excess (atom %; mean ± SE) in *Betula ermanii*-soil system: **a** leaves, **b** twigs, **c** fine roots, and **d** soil during the chase period (n = 4 per elevation). * denotes significant differences ($p < 0.05$) between the 1700 m and 2000 m plots.
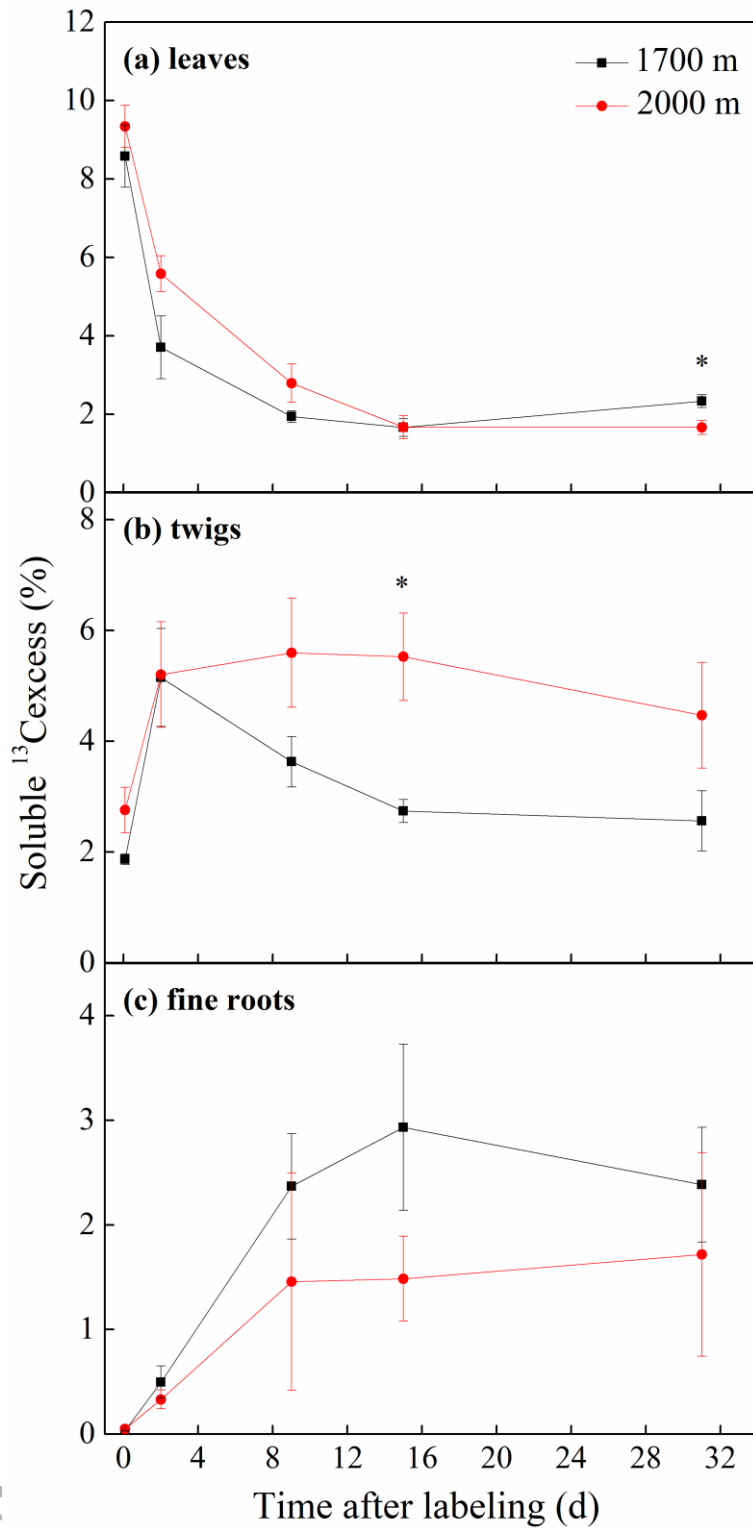
Fig. 5. Temporal variation of soluble ^{13}C excess (%; mean ± SE) in *Betula ermanii*: **a** leaves, **b** twigs and **c** fine roots during the chase period (n = 4 per elevation). * denotes significant differences ($p < 0.05$) between the 1700 m and 2000 m plots.
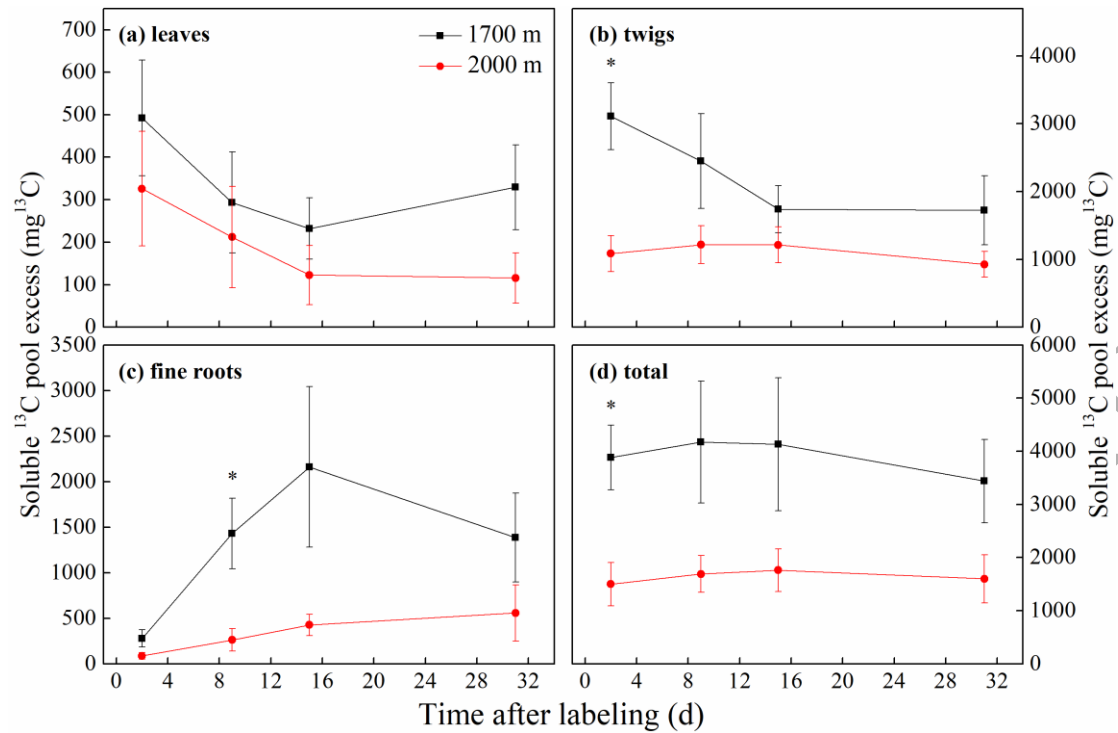
Fig. 6. Temporal variation of soluble ^{13}C excess pool (mg ^{13}C; mean ± SE) in *Betula ermanii* compartments: **a** leaves, **b** twigs, **c** fine roots, and **d** total pools during the chase period (n = 4 per elevation). * denotes significant differences ($p < 0.05$) between the 1700 m and 2000 m plots.
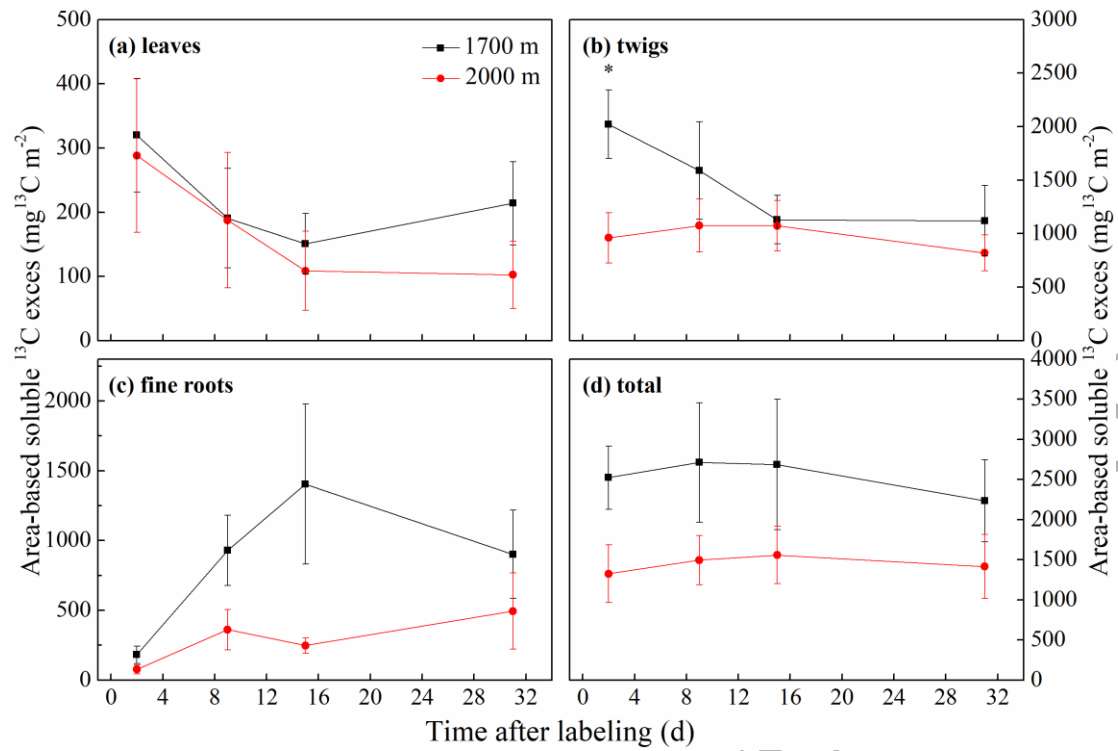
Fig. 7. Temporal variation of soluble ^{13}C excess per projected area (mean $\pm$ SE; mg^{13}C m^{-2}) in *Betula ermanii*: **a** leaves, **b** twigs, **c** fine roots, and **d** total pools during the chase period (n=4 per elevation).
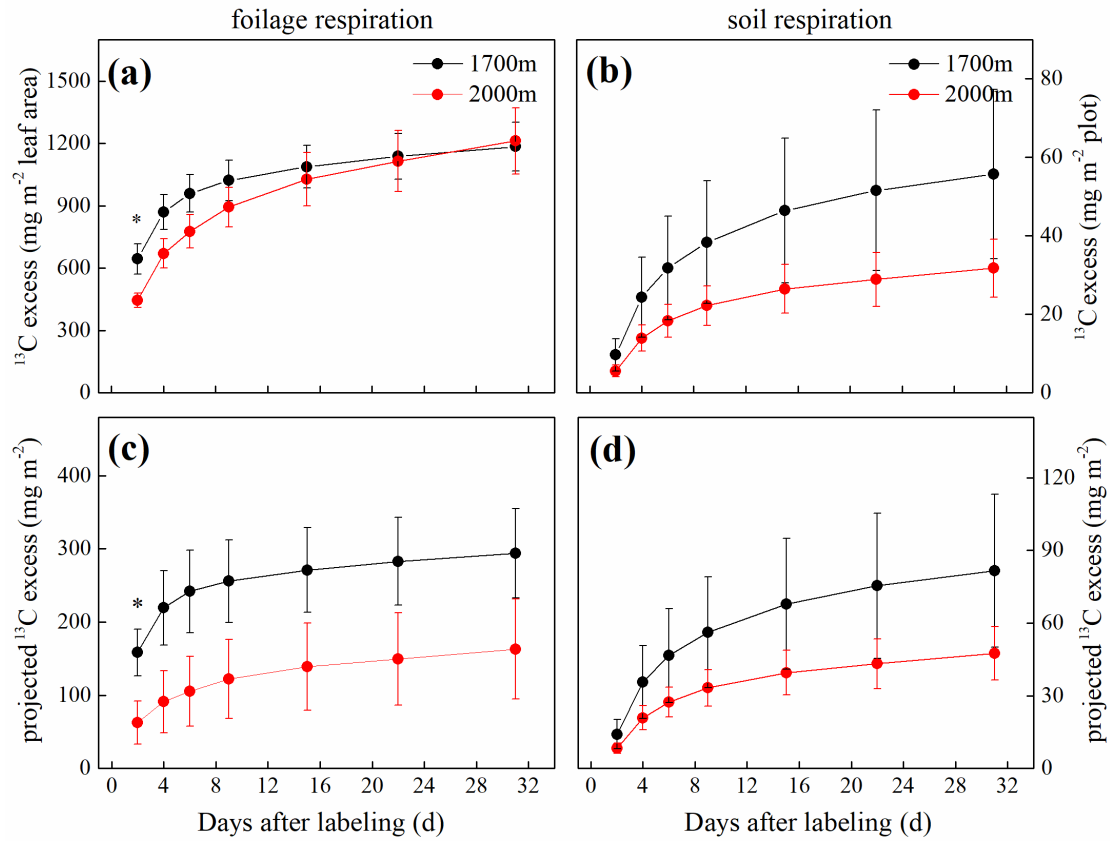
Fig. 8. ^{13}C loss (mean ± SE; n = 4 per elevation) of foliage respiration on the basis of leaf area (a) or projected ground surface area (c), ^{13}C loss of soil respiration based on plot are (b) or projected ground surface area (d) in relation to time following *Betula ermanii* labelling. * denotes significant differences ($p < 0.05$) between the 1700 m and 2000 m plots.

Table 1. Size, age and biomass of pulse-labeled *Betula ermanii* Cham. trees. Values are means (n = 4) and standard errors. Different lower-case letters within each row indicate a significant difference at $p < 0.05$ between the 1700 m and 2000 m plots (*T*-test).

Characteristic	Low-elevation	Treeline
Elevation (m)	1700	2000
Base diameter (cm)	3.50 ± 0.06^a	2.74 ± 0.09^b
Height (m)	2.27 ± 0.16^a	1.35 ± 0.11^b
Age	11.8 ± 1.7^a	12.3 ± 1.4^a
Total tree biomass (g)	704.9 ± 126.8^a	257.0 ± 68.7^b
LMA (g m^{-2})	73.55 ± 4.84^a	82.80 ± 3.36^a
Total leaf area (m^2)	0.41 ± 0.13^a	0.17 ± 0.08^a
Root-shoot ratio	0.25 ± 0.05^b	0.40 ± 0.03^a

Table 2. Maximum photosynthetic rate (A_{max}) and stomatal conductance (gs) measured on leaves of randomly selected *Betula ermanii* trees from 24 July to 1 August, and tissue mean concentration (% in dry matter) of non-structural carbohydrate (NSC) measured in samples taken from the labelled *B. ermanii* trees at 2, 9, 15 and 31 day after ^{13}C labeling ($n = 4$) in low-elevation (1700 m) and treeline (2000 m) plots. Values are given in "mean ± SE". *T*-test was used to detect differences at $p < 0.05$ between the 1700 m and 2000 m plots.

	Low-elevation (1700 m a.s.l.)	Treeline (2000 m a.s.l.)	*P*-value
A_{max} (μmol m^{-2} s^{-1})	10.00 ± 0.43	13.70 ± 1.00	0.013
gs (mmol m^{-2} s^{-1})	159.67 ± 13.69	280.67 ± 17.07	0.005
Leaf NSC (%)	21.2 ± 0.7	23.2 ± 0.7	n.s.
Twig NSC (%)	11.2 ± 0.5	11.3 ± 0.4	n.s.
Fine root NSC (%)	7.8 ± 0.4	9.4 ± 0.4	< 0.05

45

Table 3. Carbon mean residence time (MRT) ($N(t) = N_0 e^{(-\lambda t)}$, MRT $= 1/\lambda$) and coefficient of determination (R^2) from the exponential decay function of ^{13}C excess (%) in *Betula ermanii* leaves during the 31-day after the pulse labelling in low-elevation (1700 m) and treeline (2000 m) plots (n = 4 per elevation).

Elevation (m a.s.l.)	λ	MRT (d)	R^2
1700	0.101 ± 0.04	9.9	0.66
2000	0.052 ± 0.02	19.2	0.66